A Techno-Economic Analysis of Coupling Enhanced Hydrocarbon Recovery and CO_2 Storage in Gas Condensate Reservoirs

Jo Ann Tan[1,2], Guy Allinson[1,2] & Yildiray Cinar[1,2]

[1] The School of Petroleum Engineering, University of New South Wales, Sydney, Australia

[2] Cooperative Research Centre for Greenhouse Gas Technologies, Sydney, Australia

Correspondence: Guy Allinson, The School of Petroleum Engineering, University of New South Wales, Sydney NSW 2052, Australia; Cooperative Research Centre for Greenhouse Gas Technologies, Sydney NSW 2052, Australia. Tel: 61-2-9385-5296. E-mail: g.allinson@unsw.edu.au

Abstract

Coupling enhanced gas (EGR) and condensate (ECR) recoveries with CO_2 storage could potentially maintain fossil fuel supply and reduce CO_2 emissions to the atmosphere. This paper evaluates the techno-economic potential of simultaneous EGR, ECR and CO_2 storage in gas condensate reservoirs. We demonstrate that, for a closed gas condensate reservoir, injecting CO_2 later in production life is more profitable than early injection. This is because it delays CO_2 breakthrough at the production wells while enhancing gas and condensate production. In contrast, for a bottom-water drive gas condensate reservoir, we find that early CO_2 injection minimises water influx from the underlying aquifer. This maximises incremental gas and condensate production and CO_2 storage in the reservoir.

Keywords: enhanced gas recovery, enhanced condensate recovery, CO_2 storage, gas condensate reservoir, techno-economic modelling

1. Introduction

Burning fossil fuel emits CO_2, a greenhouse gas. Increased atmospheric concentration of CO_2 as a result and its link to climate change has led to the development of carbon capture and storage (CCS). CCS involves capturing CO_2 at a stationary source, compressing, transporting and finally injecting it into a suitable storage site (Benson, 2004). Among suitable storage sites, geological formations offer great potential. Such formations are (a) oil and gas reservoirs that are depleted or under enhanced gas recovery (EGR) or enhanced oil recovery (EOR) processes, (b) deep saline aquifers and (c) deep un-mineable coal beds with or without coal bed methane.

CCS is an expensive process and presently it is unclear who is going to pay for it. Current commercial CCS projects are relying on revenues from selling natural gas or crude oil. There are two cases: In the first, CO_2 is captured from high-CO_2 content gas stream and injected into a saline formation (The Sleipner and In-Salah Projects are good examples). In the second, CO_2 is captured from a point source (e.g. coal-fired power plant) or produced from a natural source and injected to an oil field for EOR (The Weyburn Project is a good example). There has also been interest in looking at gas reservoirs to assess their potential (Khan et al., 2012; Tan et al., 2012), however, because of low gas prices and high primary recoveries from gas reservoirs, this interest has been very limited. Some studies have shown that depleted gas reservoirs offer the highest CO_2 storage capacity as opposed to producing or new fields (Mamora & Seo, 2002; Oldenburg, 2003). Several recent studies (Ramharack et al., 2010; Clemens et al., 2010) have demonstrated that gas condensate reservoirs that contain both gas and liquid condensate may cover the cost of CO_2 injection and make CO_2 storage viable because of high condensate prices and incremental condensate recovery.

In a gas condensate reservoir, production causes reservoir pressure to decline. When the fluid dew point pressure is reached, the heavier hydrocarbons condense. This creates a liquid-gas region in the reservoir that decreases gas mobility. Gas production eventually stops, a condition known as condensate blockage (Fen et al., 2005). Conventional condensate blockage alleviation methods include hydraulic fracturing and recycling lean gas produced from the reservoir (Kenyon, 1987; Fen et al., 2005; Nagy et al., 2008). Experimental and numerical studies have suggested that injecting pure methane, nitrogen and supercritical CO_2 may replace the recycled lean

gas (Zaitsev et al., 1996; Al-Abri & Amin, 2009; El-Banbi, 2010). Pure supercritical CO_2 leads to the highest incremental production (Zaitsev et al., 1996; Al-Abri & Amin, 2009). This is because supercritical CO_2 is denser than reservoir gas and enables gravity-stable displacement (Shtepani, 2006; Al-Abri & Amin, 2009).

Analytical and numerical models in the literature demonstrate that CO_2 injection yields high recovery efficiency in gas condensate reservoirs at a reservoir pressure well below the dew point pressure of the initial reservoir fluid (Nagy et al., 2008). The fairly low miscibility pressure makes mature condensate reservoirs suitable targets for CO_2 storage. However, this may be offset by a possible increase in condensate recovery.

The literature tends to focus either on maximising incremental production or on CO_2 storage capacity. However, simultaneous enhanced gas recovery (EGR), enhanced condensate recovery (ECR) and CO_2 storage may be feasible (Oldenburg, 2003; Oldenburg et al., 2004; Ramharack et al., 2010; Clemens et al., 2010). Following the European Trading Scheme, commercialising simultaneous EGR, EGR and CO_2 storage for all gas reservoirs is now being considered.

In this paper, we examine how CO_2 storage can be coupled with EGR and ECR in a gas condensate reservoir. We aim to demonstrate when it is best to start CO_2 injection with given reservoir and economic conditions.

2. Methodology

2.1 Reservoir Modelling

We simulate the physical behaviour of a hypothetical, isotropic and homogeneous gas condensate reservoir. The reservoir model has characteristics and fluid compositions that reflect on the data collected from the basins located in the north-western offshore of Australia (Felton et al., 1992). The reservoir is 2.5 km subsea with a water depth of 100 m. The initial reservoir pressure is 24.5 MPa. The reservoir has an irreducible water saturation of 16%. The reservoir's temperature, porosity and permeability are 93 ^{o}C, 20% and 200 md, respectively.

We perform reservoir simulation using an academic license of Computer Modelling Group's compositional simulator, GEM. Our model is three dimensional and contains 9,800 grid blocks (N_x =35, N_y = 35 and N_z = 8). Each cell has a size of 143 m by 143 m by 12.5 m. This gives a reservoir that has an area of 2.5 km^2 and is 100 m thick.

We consider two reservoir fluids in order to assess the impact of existing CO_2 in reservoirs. The motivation for this comes from the fact that, in the Asia-Pacific region including Australia, there are many reservoirs that contain high CO_2 content. Table 1 summarises the reservoir fluid data, which are hypothetical but representative for the data collected from real reservoirs. Figure 1 shows the reservoir fluid phase diagrams for fluids with (a) no CO_2 and (b) a large amount of CO_2. We generate phase diagrams with a pressure-volume-temperature simulator. Figure 1 indicates that, at initial reservoir conditions, the reservoir fluids are in a gaseous phase.

Table 1. Reservoir fluid data

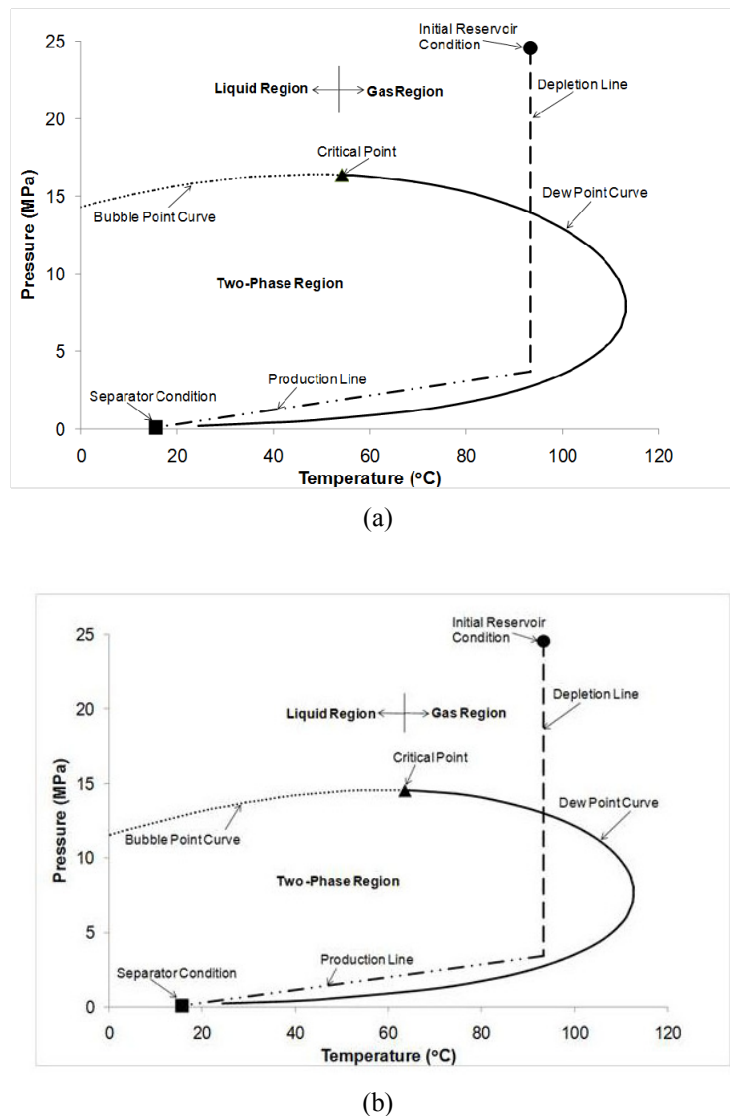| Type of Reservoir Fluids	No existing CO_2	With existing CO_2
CH_4 (mol %)	66	49
CO_2 (mol %)	0	17
C_2-C_4 and N_2 (mol %)	22	22
C_{5+} (mol %)	12	12
Original gas in place, C_1-C_4 components (x10^9 m^3) [10^{12} scf]	85 [3]	85 [3]
Original condensate in place, C_{5+} components (10^6 m^3) [10^6 STB]	40 [250]	40 [250]
Dew point pressure (MPa)	15	13

(a)

(b)

Figure 1. Reservoir fluid phase diagram, (a) fluid with no existing CO_2, (b) fluid with existing CO_2 volume

We examine both closed and bottom-water drive gas condensate reservoirs. Both reservoirs have the same reservoir and fluid data. We neglect capillary pressure effects as they are negligible during production. The difference between closed and bottom-water drive gas condensate reservoirs lies in their fluid phase behaviour during production. Condensate and gas production in a closed gas condensate reservoir causes reservoir pressure to decline at almost isothermal conditions. When reservoir pressure drops below the dew point, heavier hydrocarbons condense into liquid condensate and they form a liquid phase. The system becomes a two-phase system and gas mobility decreases. Gas mobility can be defined by k_{rg}/μ_g where k_{rg} is the gas relative permeability and μ_g is the gas viscosity. Figure 2(a) shows data for liquid-gas relative permeability. We take this data from the gas condensate model of the third comparative solution project presented by the Society of Petroleum Engineers (SPE) (Kenyon, 1987). Above the dew point pressure, the reservoir is saturated with gas only. Therefore, the gas saturation (S_g) equals to one and $k_{rg}=1$. Below the dew point, the reservoir is saturated with both liquid and gas. The volume conservation in the reservoir suggests that the sum of liquid and gas saturation must equal to one. As S_g decreases k_{rg} goes towards zero. See Figure 2(b).

Condensate and gas production in a bottom-water drive gas condensate reservoir causes moderate pressure decline. Water from the underlying aquifer moves into the reservoir and this maintains reservoir pressure above the dew point. Therefore, no heavier hydrocarbons condense and only water and gas form separate phases in the reservoir. The presence of water in pore space affects the flow of gas. First of all, it shares pore space with gas and this decreases gas mobility. Secondly, water wets the rock in preference to gas and water influx to the

reservoir leads to gas snap-off, trapping a residual gas in the water-flooded zone.

We simulate gas entrapment using the imbibition relative permeabilities. We calculate imbibition relative permeabilities using Land's model (Land, 1968). Figure 2(b) shows the gas-water relative permeabilities. Appendix A summarises the equations in Land's model. The calculation of relative permeabilities assumes 84% for the initial gas saturation, 35% for the maximum trapped residual gas saturation and 3 for the pore distribution parameter (ε).

2.2 Economic Modelling

Our economics model incorporates a simple taxation scheme. We estimate capital expenditure (CAPEX) based on that of an existing gas condensate field. The field development CAPEX includes the cost of capturing CO_2 (Al-Hassami et al., 2005). We estimate CO_2 injection costs using an in-house CCS cost estimating model (Allinson et al., 2006). The assumptions used are highlighted in Appendix B.
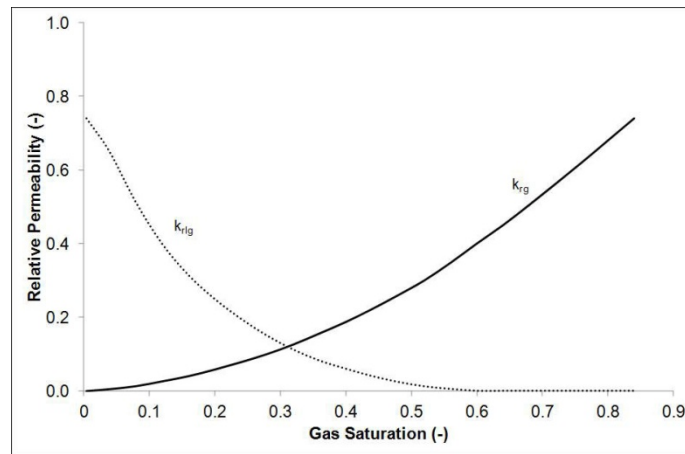
Figure 3 shows the system boundary for our economic model. It highlights the revenue obtained from producing methane and gas condensate and injecting CO_2. It also shows the penalty for emitting CO_2 emission.

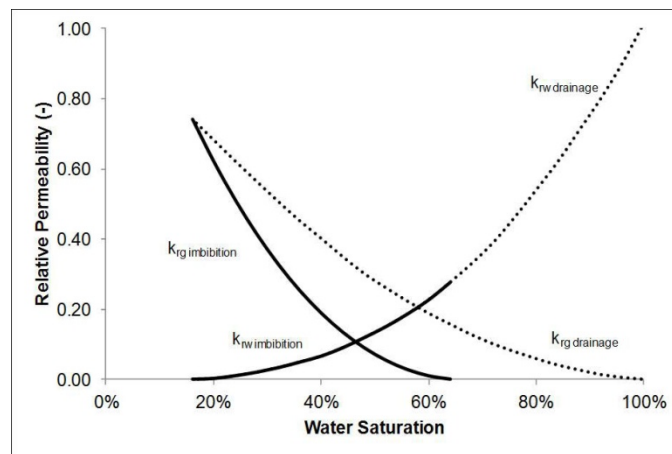### 2.3 Co-Optimisation Evaluation

Reservoir conditions affect the field development strategy and development's net present value (NPV). Field development strategy is an optimised combination of field development parameters. These development parameters are well numbers, well perforation interval, production rate, injection rate, well bottom-hole pressure (BHP) and injection starting time. The NPV is the present value of the sum of future after tax cash flow. The optimal development strategy is that which maximises the NPV for simultaneous EGR, ECR and CO_2 storage.

We evaluate injecting CO_2 for four scenarios. These are

      A. Primary depletion. These cases do not involve CO_2 injection;

      B. Injection at the start of production. These cases involve injecting CO_2 from the start of production;

      C. Injection during production. These cases involve injecting CO_2 during production and before the end of primary depletion;

      D. Injection at the end of primary depletion economic life. These cases involve injecting CO_2 following the end of the economic life based on primary depletion.

(a)

(b)

Figure 2. Relative permeabilities, (a) closed gas condensate reservoir gas-liquid condensate, (b) bottom-water drive gas condensate reservoir gas-water
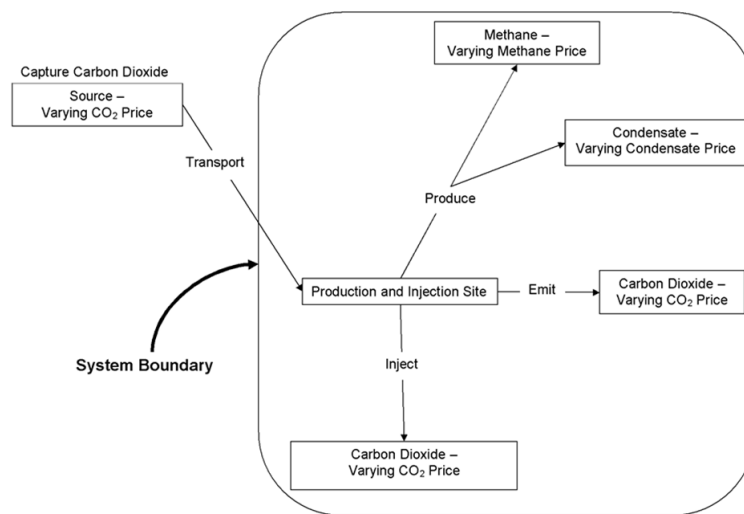

Figure 3. Economics model system boundary

Each injection scenario has different optimal field development parameters. It is important first to optimise each injection scenario before making comparisons between them. This is because each field development parameter affects the NPV differently at different reservoir conditions and production maturity.

Analytical constraints are placed to simplify the evaluation. These constraints are

- Vertical injection and production wells only;

- Each injection well injects up to 1million tones of CO_2 per annum (Mtpa);

- Injection takes a maximum of 25 years;

- Methane and gas condensate production must be at least 15 years.

3. Results

3.1 Closed Reservoirs

Figure 4 shows the maximum NPV for each injection scenario at their respective optimal field development strategy for fluids with (a) no CO_2 and (b) significant existing CO_2. Table C-1 in Appendix C summarises the optimal field development parameters for each injection scenario. Figure 4 shows that CO_2 injection during production is the most profitable. For the reservoir fluid without existing CO_2, the optimal field development strategy is with CO_2 injection from year 6 of production. See Appendix C. This is later than year 3 of production in the bottom-water drive gas condensate reservoir. The same goes for the reservoir fluid with existing CO_2, which has CO_2 injection starting year 9 of production for the closed gas condensate reservoir. This is later than year 4 as is the case with the bottom-water drive gas condensate reservoir. These comparisons suggest that delaying CO_2 injection is preferable. This is because delayed CO_2 injection delays CO_2 breakthrough while maintaining the reservoir pressure. This prolongs fluid mobility and production.

In the closed gas condensate reservoir, the reservoir pressure declines when production begins. When the reservoir pressure drops below the dew point pressure, the heavier hydrocarbons condense into condensate. This creates two-phase flow, which decreases gas mobility. Figure 5 shows the interfacial tension (IFT) profile for each injection scenario over time for the reservoir fluid with no existing CO_2. The trends are similar for both reservoir fluids with and without existing CO_2.

During production the volume of hydrocarbons in the reservoir decreases. Lighter hydrocarbons flow faster than heavier hydrocarbons. Therefore, the rate of production of each component is different. This changes the overall reservoir fluid composition, which in turn alters the dew point. Figure 6 shows the average reservoir pressure and dew point profiles for the reservoir fluid with no existing CO_2. Table 2 shows the variation of overall reservoir fluid composition over the production life of the field.

During primary depletion, reservoir pressure falls and increases liquid condensate saturation. This raises liquid-gas IFT and hinders production.
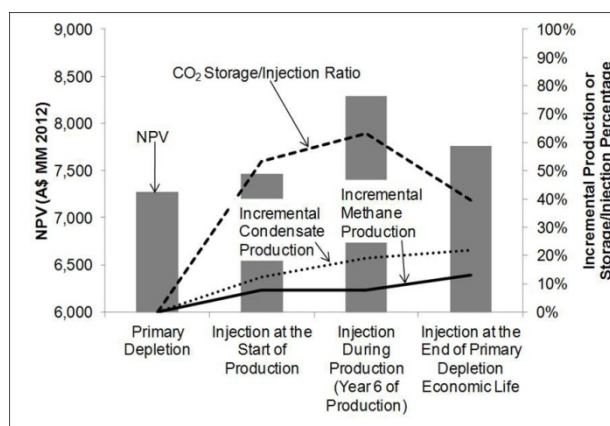
Injecting CO_2 at the start of production requires a low injection rate to delay CO_2 breakthrough and maximise the NPV. A low injection rate delays the reservoir pressure decline and increases the liquid-gas IFT. See Figure 5 and Figure 6(a). CO_2 injection also changes fluid composition and decreases the reservoir fluid's dew point. See Figure 6(b). Varying the dew point pressure alters the condition at which heavier hydrocarbons change phase. At a high production rate, the average reservoir pressure declines faster than the fluid's dew point pressure decline induced by the change in reservoir fluid composition. Therefore the reservoir pressure eventually approaches the dew point and then heavier hydrocarbons condense and the liquid-gas IFT increases. This leads to condensate blockage around the wells and consequently a decrease in gas relative permeability. The gas production rate declines as a result. However, delaying the decline in reservoir pressure prolongs gas mobility and increases hydrocarbon recovery.

Injection during production has the highest NPV when CO_2 injection begins in Year 6 of production. A high injection rate is required to maintain reservoir pressure and avoid condensate blockage. See Figure 6(a). A high CO_2 injection rate causes a rapid increase in CO_2 concentration in the reservoir fluid. This causes the reservoir fluid dew point to decrease. As the dew point declines faster and the reservoir pressure is maintained above the dew point, heavier hydrocarbons always stay in the gaseous phase. See Figure 6. As the heavier hydrocarbons do not condense and the liquid-gas IFT is always zero. See Figure 5. This avoids condensate blockage and aids incremental condensate and gas production.
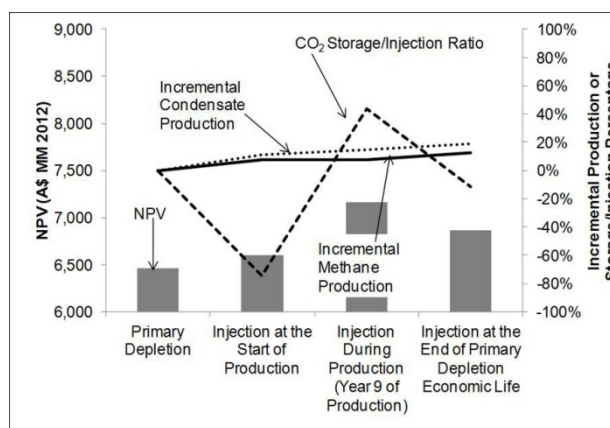
Condensate blockage occurs during primary depletion. Figure 5 shows that the liquid-gas IFT increases as production starts. At the end of primary depletion, the reservoir has a high concentration of heavier hydrocarbons. This causes the fluid dew point to increase. See Figure 6(b). CO_2 injection at the end of primary depletion raises

the reservoir pressure. See Figure 6(a). It also increases CO_2 concentration in the fluid and decreases the fluid dew point. The combined effects of the increase in reservoir pressure and the decrease in fluid dew point decrease the liquid-gas IFT and improve fluid mobility. See Figure 5. This alleviates condensate blockage and aids incremental condensate and gas production.

Figure 4 also shows the incremental production compared to that of primary depletion and CO_2 storage-on-injection (storage/injection) ratio. Delayed CO_2 injection avoids condensate blockage. Therefore condensate and methane production is maintained. Figure 4 shows that injecting CO_2 during production leads to lower incremental methane recovery than injecting CO_2 at the start or end of production. This is because a high CO_2 injection rate causes CO_2 and methane production to compete.

(a)

(b)

Figure 4. Closed gas condensate reservoir overall NPV, incremental production and CO_2 storage/injection ratio, (a) fluid with no existing CO_2, (b) fluid with existing CO_2 volume
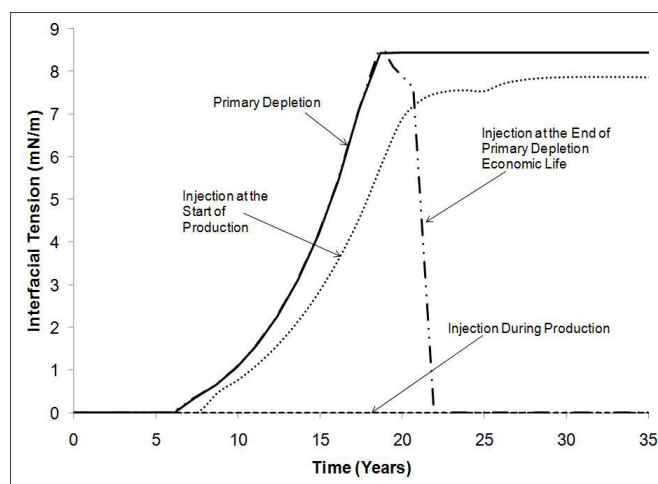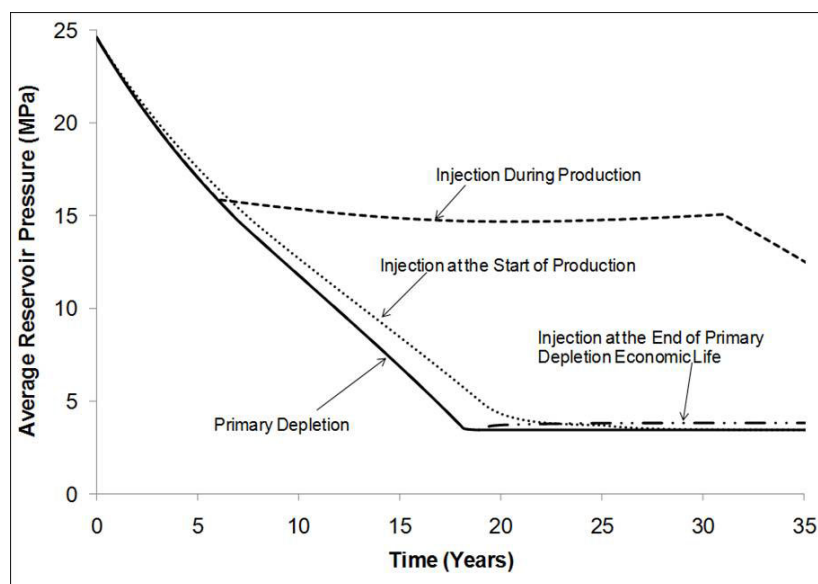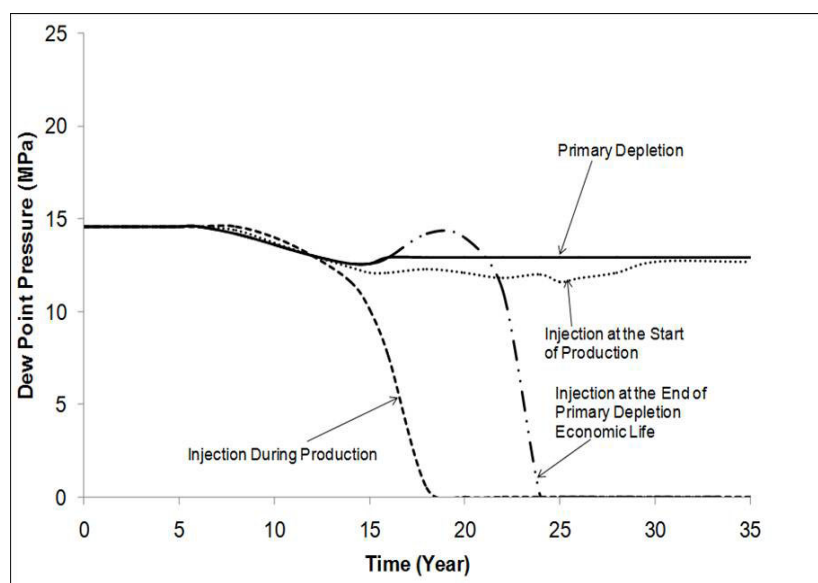
Figure 5. Closed gas condensate reservoir liquid condensate-gas interfacial tension profile for fluid with no existing CO_2

Table 2. Reservoir gas composition for a reservoir fluid with no existing CO_2

Case	Time (years)	C_1 (mol%)	C_{2-4}, N_2 (mol %)	CO_2 (mol %)	C_{5+} (mol%)
Initial conditions	0	66	22	0	12
Primary depletion	10	68	22	0	10
	20	68	23	0	9
	30	68	23	0	9
Injection at the start of production	10	67	21	1	11
	20	50	17	23	10
	30	48	17	25	10
Injection during production	10	61	21	7	11
	20	21	7	68	4
	30	3	2	94	1
Injection at the end of primary depletion economic life	10	68	22	0	10
	20	60	21	7	12
	30	0.05	0.05	99.8	0.1

(a)

(b)

Figure 6. Closed gas condensate reservoir and fluid with no existing CO_2 (a) average reservoir pressure profile, (b) fluid dew point pressure profile

Figure 4(a) shows that injection at the end of production lowers CO_2 storage. This is because CO_2 injection experiences an immediate CO_2 breakthrough in depleted reservoirs. The same phenomenon is noted by Jikich et al. (2003) on CO_2 injection into a gas reservoir. This lowers CO_2 storage capacity and gives a lower storage/injection ratio.

Figure 4(b) shows that, with injection at the start and at the end of production, the CO_2 storage/injection ratios are negative. This is because the CO_2 production rate is higher than the CO_2 injection rate. Our assumptions and constraints show that delaying CO_2 injection benefits the NPV, condensate and gas production and CO_2 storage capacity. However, it is better to inject CO_2 before the reservoir is depleted.

3.2 Bottom-Water Drive Reservoirs

Figure 7 shows the NPV for each injection scenario with optimal field development strategies with and without existing CO_2. Table C-2 in Appendix C summarises the optimal field development parameters for each injection

scenario. Figure 7 shows that it is most profitable to inject CO_2 during production. In fact, CO_2 injection should start in year 3 and year 4 of production for reservoir fluids without and with existing CO_2, respectively. These injection starting times are earlier than the optimal injection starting years for the closed gas condensate reservoir, which are year 6 and 9. This suggests that it is better to commence CO_2 injection early in the production phase. This is because early CO_2 injection minimises water influx into the reservoir from the underlying aquifer. It maintains gas mobility and prolongs production. Figure 8 shows the average reservoir pressure profile for the reservoir fluid with no existing CO_2. It is clear that the reservoir pressure remains above the dew point during production. The trends are similar for the reservoir fluids with and without existing CO_2.

Gas production declines because water influx raises water saturation and lowers the effective gas permeability significantly. Gas trapped in the water-flooded region of the reservoir causes gas mobility and production to decrease (Lyons & Plisga, 2005). Figure 9 shows the gas permeability profile. The trends are similar for both reservoir fluids. Early CO_2 injection delays or alleviates the decline in gas permeability. Gas permeability reaches a minimum when we inject CO_2 at the end of primary depletion. This is because CO_2 injection raises gas saturation, permeability and mobility.

Figure 7 shows the relative incremental production and CO_2 storage/injection percentages for each injection scenarios. Early CO_2 injection leads to higher incremental recoveries. This is because it minimises water influx and gas entrapment. This aids gas mobility and prolongs production.

For the reservoir fluid with no existing CO_2, the CO_2 storage/injection ratio is higher when CO_2 injection starts early production. See Figure 7(a). This is because early CO_2 injection introduces CO_2 into the gaseous region of the reservoir. It also stops water from moving into the top of the reservoir. Reservoir gas has a density of about 200 kg/m^3, while the supercritical CO_2 density is approximately 600 kg/m^3. Denser supercritical CO_2 sinks to the bottom of the reservoir and makes reservoir gas displacement gravity-stable. Therefore, early CO_2 injection during production stores more CO_2 than delayed CO_2 injection.

Furthermore, at the end of primary depletion, water will have flooded most of the reservoir and CO_2 will be injected into water-invaded zones. Injecting CO_2 into water-invaded zones causes CO_2 preferential flow. This is because of the difference in viscosities between CO_2 and water. CO_2 flows as a plume in water-invaded zones, causing viscous fingering and an unstable displacement front. This raises methane and gas condensate production slightly, but CO_2 breakthrough occurs at higher concentrations.

For the reservoir fluid with existing CO_2 concentration, the CO_2 storage/injection ratio is higher when CO_2 injection is delayed. See Figure 7(b). This is because early CO_2 injection causes incremental CO_2 production. As the CO_2 production rate is higher than the injection rate, the storage capacity is diminished. In the cases where injection begins at the end of primary depletion, CO_2 preferential flow causes less incremental CO_2 production and gives a higher storage capacity.

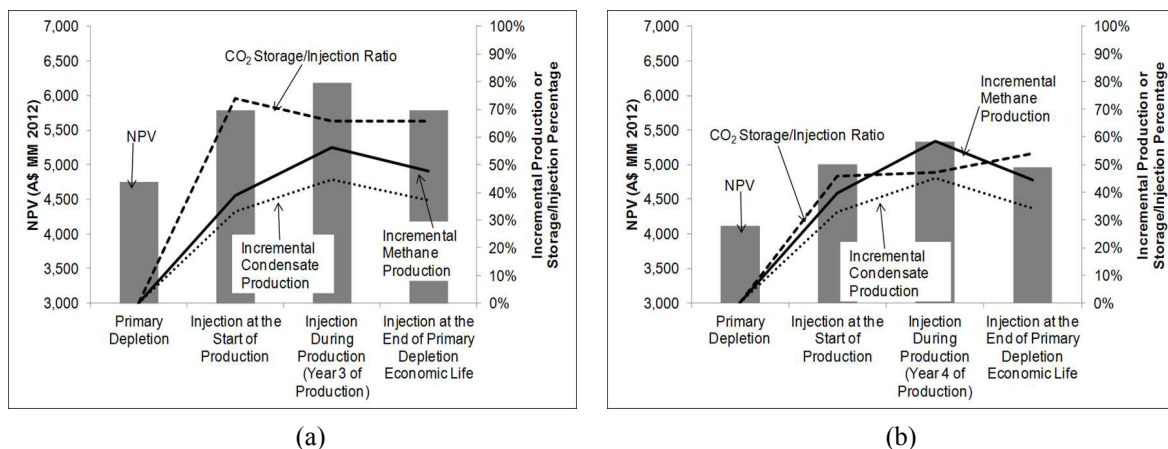(a)   (b)

Figure 7. Bottom-water drive gas condensate reservoir overall NPV, incremental production and CO_2 storage/injection ratio, (a) fluid with no existing CO_2, (b) fluid with existing CO_2 volume
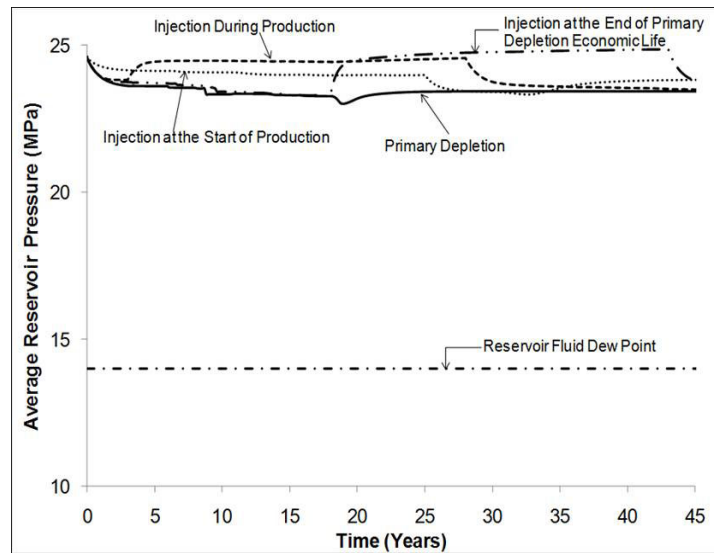
Figure 8. Bottom-water drive gas condensate reservoir average reservoir pressure for fluid with no existing CO_2 profile
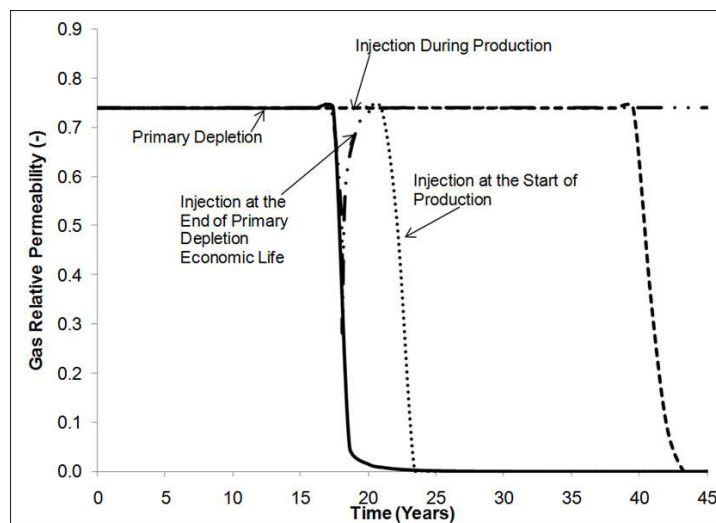

Figure 9. Bottom-water drive gas condensate reservoir gas relative permeability profile for fluid with no existing CO_2

4. Discussion

Reservoir heterogeneity affects the reservoir performance of injection processes significantly and yet this paper uses a homogeneous reservoir model for its numerical simulations. The exclusion of reservoir heterogeneity from the studies may appear to undermine the predictions made. Hence, there is a need to demonstrate whether neglecting reservoir heterogeneity might affect the results significantly.

One of the ways to assess whether the heterogeneity has an impact on the displacements that take place during injection is to understand the dominant forces in the displacements. If, for example, gravitational forces dominate the displacement, then reservoir heterogeneity can be ignored. Shook et al. (1992) described the following gravity number to assess the balance between gravitational and viscous forces during a displacement:

$$N_G = \frac{g \Delta \rho_{CO_2 / condensate}}{v_{CO_2} \mu_{CO_2}} \left(\frac{k}{\varphi} \right) \tag{1}$$

where N_G is the gravity number, g is the gravitational constant (9.8 m/s^2), $\Delta\rho$ is the density difference between the supercritical CO_2 and in-situ gas condensate (350 kg/m^3), k is the permeability (2×10^{-13} m^2), ϕ is the porosity (0.2), v is the velocity and μ is the CO_2 viscosity (5×10^{-5} Pa.s). Equation (1) suggests that, if $N_G > 1$, CO_2 injection

is governed by gravitational forces, which means that reservoir heterogeneity can be ignored. Otherwise, viscous forces dominate CO_2 injection and heterogeneity needs to be considered.

The CO_2 velocity in the reservoir varies, being highest in the vicinity of an injection well and lowest in parts of the reservoir away from the well. For the cases summarised in Appendix C, the lowest and highest injection rates per well are calculated to be 0.1 and 1 Mtpa, respectively. We calculate gravity numbers as a function of the distance from injector. Figure 10 shows the results. These indicate that, for the cases with low injection rate, CO_2 injection is mainly governed by gravity forces whereas a balance between gravity and viscous forces controls other cases. Note, however, that the simulations are run on blocks of a uniform size of 143 m which suggests that the flow in all grids other than well grids should be dominated mainly by gravitational forces for all cases. This demonstrates that the results presented in this paper should be representative of reservoirs other than the homogeneous reservoirs analysed here.
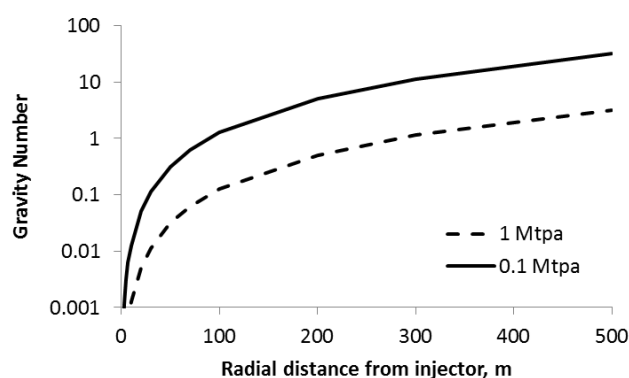

Figure 10. Gravity number as a function of the distance from injector

5. Conclusions

We have presented a techno-economic study that shows the potential of coupling enhanced gas and condensate recoveries with CO_2 storage for gas condensate reservoirs. Our analyses show that injecting CO_2 during production is the most profitable for both closed and bottom-water drive gas condensate reservoirs with and without existing CO_2. However, the optimum injection time depends on the conditions of a particular reservoir.

Our analyses show that, in closed gas condensate reservoirs, CO_2 injection should start later in production than it should in bottom-water drive gas condensate reservoirs. Delayed CO_2 injection maintains reservoir pressure and delays CO_2 breakthrough. This maximises the NPV of the project and optimises incremental production and CO_2 stored. In bottom-water drive gas condensate reservoirs, CO_2 injection should start earlier in production to minimise water encroachment from the underlying aquifer. This maximises NPV by optimising field recovery and CO_2 storage capacity.

Reservoir performance at different stages of production is influenced by different field development parameters. Therefore, it is important to optimise the field development strategy before determining the best time to inject CO_2.

Acknowledgements

Nomenclature

BHP   Bottom-hole pressure

CAPEX   Capital expenses

C_2-C_4 Ethane to butane

C_{5+} Pentane and heavier hydrocarbons

GJ   Gigajoules

IFT   Interfacial tension

Mol %	Molecular fraction
md	Millidarcy
Mt	Megatonnes
Mtpa	Megatonnes per annum
NPV	Net present value
OPEX	Operating expenses
scf	Standard cubic feet
scf/d	Standard cubic feet per day
STB	Stock tank barrel
C	Trapping characteristic constant
ε	Saturation exponent
k	Relative permeability
S	Saturation
μ	Viscosity
g	Gas
gF	Free gas (used with saturation)
gr	Residual gas (used with saturation)
gt	Trapped gas (used with saturation)
l	Liquid
w	Water
wc	Connate water (used with saturation)
*	Effective value (used with saturation)

References

Al-Abri, A. S., & Amin, R. (2009). Enhanced natural gas and condensate recovery by injection of pure $SCCO_2$, pure CH_4 and their mixtures: Experimental investigation. *SPE Annual Technical Conference and Exhibition. Society of Petroleum Engineers Inc., New Orleans, Louisiana*. Retrieved from http://www.onepetro.org/mslib/servlet/onepetropreview?id=SPE-124145-MS

Al-Hasami, A., Ren, S., & Tohidi, B. (2005). CO_2 injection for enhanced gas recovery and geo-storage: Reservoir simulation and economics. *SPE Europec/EAGE Annual Conference*. Society of Petroleum Engineers Inc., Madrid, Spain. http://dx.doi.org/10.2118/94129-MS

Allinson, G., Neal, P., Ho, M., Wiley, D., & McKee, G. (2006). *CCS economics methodology and assumptions*. Cooperative Research Centre for Greenhouse Gas technologies, Canberra, Australia.

Benson, S. M. (2004). Carbon dioxide capture and storage in underground geologic formations. The 10-50 Solution: Technologies and Policies for a Low-Carbon Future. *The Pew Centre* (p. 18). Retrieved from http://www.c2es.org/docUploads/10-50_Benson.pdf

Clemens, T., Secklehner, S., Mantatzis, K., & Jacobs, B. (2010). Enhanced gas recovery - Challenges shown at the example of three gas fields. *SPE EUROPEC/EAGE Annual Conference and Exhibition, Barcelona, Spain*. http://dx.doi.org/10.2118/130151-MS

El-Banbi, A. H. (2010). Optimizing simulation studies for gas condensate field development and management. North Africa Technical Conference and Exhibition. Cairo, Egypt: Society of Petroleum Engineers Inc. http://dx.doi.org/10.2118/128448-MS

Fan, L., Harris, B. W., Jamaluddin, A. J., Kamath, J., Mott, R., Pope, G. A., ... Whitson, C. H. (1998). Understanding gas-condensate reservoirs. *Oilfield Review, 10*(3), 16-25.

Felton, E. A., Miyazaki, A., Dowling, L., Pain, L., Vuckovic, V., & le Poidevin, S. (1992). Carnarvon Basin, W. A. in Bureau of Resource Science. Geoscience Australia (p. 259).

Jikich, S. A., Smith, D. H., Sams, W. N., & Bromhal, G. S. (2003). Enhanced gas recovery (EGR) with carbon dioxide sequestration: A simulation study of effects of injection strategy and operational parameters. *SPE Eastern Regional Meeting. Society of Petroleum Engineers, Pittsburgh, Pennsylvania*. http://dx.doi.org/10.2118/84813-MS

Kenyon, D. (1987). Third SPE comparative solution project: Gas cycling of retrograde condensate reservoirs. *Journal of Petroleum Technology, 39*, 981-97. http://dx.doi.org/10.2118/12278-PA

Khan, C., Amin, R., & Madden, G. (2012). Economic modelling of CO_2 injection for enhanced gas recovery and storage: A reservoir simulation study of operational parameters. *Energy and Environment Research, 2*(2), 65-82. http://dx.doi.org/10.5539/eer.v2n2p65

Land, C. (1968). Calculation of imbition relative permeability for two-and three-phase flow from rock properties. *Old SPE Journal, 8*(2), 149-156.

Lyons, W. C., & Plisga, G. J. (2005). Chapter 6 Production Engineering. Standard Handbook of Petroleum and Natural Gas Engineering. Gulf Professional Publishing. In E. A. Felton, A. Miyazaki, L. Dowling, L. Pain, V. Vuckovic, & S. le Poidevin (Eds.), *Carnarvon Basin, W.A. in: B.o.R. Sciences* (p. 259). Parkes, Australia: Geoscience Australia.

Mamora, D. D., & Seo, J. G. (2002). Enhanced gas recovery by carbon dioxide sequestration in depleted gas reservoirs. *SPE Annual Technical Conference and Exhibition*. Society of Petroleum Engineers Inc., San Antonio, Texas.

Nagy, G., Benedek, L., Pipicz, V., Papp, I., Hnisz, M. Ó., & Varga, I. T. (2008). Gas supply security or enhanced gas recovery? With adequate reservoir management-No need to choose! *Development, 3*, 50-62.

Oldenburg, C. M. (2003). Carbon sequestration in natural gas reservoirs: Enhanced gas recovery and natural gas storage. *Lawrence Berkeley National Laboratory*. LBNL-52476.

Oldenburg, C. M., Stevens, S. H., & Benson, S. M. (2004). Economic feasibility of carbon sequestration with enhanced gas recovery (CSEGR). *Energy, 29*(2004), 1413-1422. http://dx.doi.org/10.1016/j.energy.2004.03.075

Ramharack, R. M., Aminian, K., & Ameri, S. (2010). Impact of carbon dioxide sequestration in gas/condensate reservoirs. *SPE Eastern Regional Meeting*. Society of Petroleum Engineers, Morgantown, West Virginia, USA. http://dx.doi.org/10.2118/139083-MS

Shook, M., Li, D., & Lake, W. L. (1992). Scaling immiscible flow through permeable media by inspectional analysis. *In Situ, 16*, 211-349.

Shtepani, E. (2006). CO_2 sequestration in depleted gas/condensate reservoirs. *SPE Annual Technical Conference and Exhibition*. Society of Petroleum Engineers, San Antonio, Texas, USA.

Tan, J. A., Cinar, Y., & Allinson, G. (2012). Enhanced recovery and CO_2 storage in bottomwater drive gas reservoirs. *Eastern Australasian Basins Symp*. IV, Brisbane, QLD, 10-14 September.

Zaitsev, I. Y., Dmitrievsky, S. A., Norvik, H., Yufin, P. A., Bolotnik, D. N., Sarkisov, G. G., & Schepkina, N. E. (1996, October). Compositional modeling and PVT analysis of pressure maintenance effect in gas condensate field: Comparative study. In *European Petroleum Conference*.

Appendix A - Land's Model for Two-Phase Flow Imbibition Relative Permeabilities

We summarise the equations used in calculating water and gas imbibition relative permeabilities. The reservoir model is assumed to be homogeneous and isotropic with negligible capillary pressure effects. Hence pore size in the reservoir is the same. Therefore, the exponent of saturation (ε) is 3 (Land, 1968). The other data used to obtain Figure 2(b) is $S_{wc} = 1 - S_{gi} = 0.16$ and $S_{gr,max} = 0.35$.

$$S_g^* = \frac{S_g}{1 - S_{wc}} \tag{A.1}$$

$$S_w^* = \frac{S_w - S_{wc}}{1 - S_{wc}} \tag{A.2}$$

$$C = \frac{1}{S_{gr\,max}^*} - 1 \tag{A.3}$$

$$S_{gr}^* = \frac{S_{gi}^*}{1 + CS_{gi}^*} \tag{A.4}$$

$$S_{gF}^* = \frac{1}{2}\left[(S_g^* - S_{gr}^*) + \sqrt{(S_g^* - S_{gr}^*)^2 + \frac{4}{C}(S_g^* - S_{gr}^*)} \right] \tag{A.5}$$

$$k_{r,imbibition} = (S_{gF}^*)^2 \left[1 - (1 - S_{gF}^*)^{\varepsilon-2} \right] \tag{A.6}$$

$$S_{gt}^* = S_{gr}^* - \frac{S_{gF}^*}{1 + CS_{gF}^*} \tag{A.7}$$

$$k_{rw,imbibition} = (S_w^*)^4 + (S_w^*)^2 \left[\left(2S_w^* + S_{gt}^* - \frac{2}{1 - S_{gr,max}} \right) S_{gt}^* - \frac{2}{C^2} \ln\left(\frac{(S_{gr,max}^2)^2 (S_w^* + S_{gt}^*)}{S_{gt}^*} \right) \right] \tag{A.8}$$

However, if $\varepsilon = 3$, Equation (A.8) can be simplified to

$$k_{rw,imbibition} = k_{rw,drainage} + fn(S_w^*) \tag{A.9}$$

where the condition that $fn(S_w^*) = 0$ represents a homogeneous and isotropic reservoir.

Appendix B – Economic Model Assumptions

This appendix refers to Section 2.2. Our economic model assumptions (Allinson et al., 2006).

Table B-1. Economic model assumptions

Item	Value/ Description
Historical CAPEX unit cost	17.25
(A$ 2010/ 106 scfd raw gas)	
Capacity scaling factor (%)	70
CAPEX instalment payment (%)	40 in first year
	60 in second year
Depreciation method	Straight line
Depreciation rate (%)	20
OPEX (% of CAPEX)	5
Annual operation period (days)	365
Inflation rate (%)	3
Discount rate (%)	10
Income tax rate (%)	40
Methane price (A$ /GJ)	5
Condensate price (A$ /STB)	70
CO_2 price (A$ /tonne)	25

Appendix C – Optimal Field Development Strategies

Table C-1. Closed gas condensate reservoirs

Type of Fluid	No existing CO_2				Existing CO_2			
Injection strategies	A	B	C	D	A	B	C	D
Flooding pattern	Square	Inverted 5-spot	Inverted 9-spot	Inverted 9-spot	Square	Inverted 5-spot	Inverted 9-spot	Inverted 9-spot
Well numbers (Production : injection)	49:0	16:9	40:9	40:9	49:0	16:9	40:9	40:9
Production well perforation depth (m, from top of the reservoir)	94	6	6	6 and 94	94	6	6	6 and 94
Production well perforation thickness (m)	24	6	6	6	24	6	6	6
Injection well perforation depth (m, from top of the reservoir)	-	6	94	61	-	6	94	61
Injection well perforation thickness (m)	-	6	6	6	-	6	6	6
Total production rate (10^6 m^3/d) [10^6 scf/d]	11 [400]	11 [400]	11 [400]	11 [400]	11 [400]	11 [400]	11 [400]	11 [400]
Total injection rate (Mtpa)	-	1	9	4	-	1	9	4
Production well maximum BHP (MPa)	3	3	14	3	3	3	14	3
Injection well minimum BHP (MPa)	-	32	32	32	-	32	32	32
Injection starting time (Year of production)	-	1	6	19	-	1	9	20
Cumulative CH_4 production (10^9m^3) [10^{12} scf]	76 [2.7]	82 [2.9]	82 [2.9]	85 [3.0]	65 [2.3]	70 [2.5]	70 [2.5]	73 [2.6]
Cumulative condensate production (10^6m^3) [10^6 STB]	29 [182]	33 [207]	35 [220]	35 [220]	31 [195]	34 [214]	35 [220]	36 [226]
Cumulative CO_2 injected (Mt)	-	23	217	62	-	40	217	58
Cumulative CO_2 stored (Mt)	-	12	137	25	-27	-17	95	-7

(Injection strategies: A – primary depletion, B – injection at the start of production, C – injection during production, D – injection at the end of primary depletion economic life)

Table C-2. Bottom-water drive gas condensate reservoirs

	No existing CO_2				With existing CO_2			
Injection strategies	A	B	C	D	A	B	C	D
Flooding pattern	Square	Inverted 5-spot	Inverted 9-spot	Inverted 9-spot	Square	Inverted 5-spot	Inverted 9-spot	Inverted 9-spot
Well numbers (Production : injection)	49:0	21:4	40:9	40:9	49:0	21:4	40:9	40:9
Production well perforation depth (m, from top of the reservoir)	6	6	6	6 and 94	6	6	6 and 94	6
Production well perforation thickness (m)	6	6	6	6	6	6	6	6
Injection well perforation depth (m, from top of the reservoir)	-	6	6	94	-	6	61	94
Injection well perforation thickness (m)	-	6	6	6	-	6	24	6
Total production rate (10^6 m^3/d) [10^6 scf/d]	7 [250]	7 [250]	7 [250]	7 [250]	7 [250]	7 [250]	7 [250]	7 [250]
Total injection rate (Mtpa)	-	4	7	9	-	4	7	9
Production well maximum BHP (MPa)	21	21	21	21	21	21	21	21
Injection well minimum BHP (MPa)	-	32	32	32	-	32	32	32
Injection starting time (Year of production)	-	1	3	18	-	1	4	19
Cumulative CH_4 production (10^9m^3) [10^{12} scf]	45 [1.6]	65 [2.3]	73 [2.6]	68 [2.4]	39 [1.4]	56 [2.0]	62 [2.2]	56 [2.0]
Cumulative condensate production (10^6m^3) [10^6 STB]	21 [132]	28 [176]	31 [195]	29 [182]	21 [132]	28 [176]	31 [195]	29 [182]
Cumulative CO_2 injected (Mt)	-	93	168	217	-	93	169	216
Cumulative CO_2 stored (Mt)	-	68	110	142	-17	43	80	117

(Injection strategies: A – primary depletion, B – injection at the start of production, C – injection during production, D – injection at the end of primary depletion economic life)

Copyrights